

Nature of the E - B decomposition of CMB polarization

Matias Zaldarriaga

Physics Department, New York University, 4 Washington Place, New York, New York 10003

(Received 10 June 2001; published 3 October 2001)

We present a derivation of the transformation between the Q and U Stokes parameters and the E and B scalar and pseudoscalar fields. We emphasize the geometrical properties that such transformation must satisfy. We present the E and B decompositions of some simple maps and of a model for a supernova remnant. We discuss the relative amplitudes of the E and B components, and argue that for generic random maps E and B should have roughly the same amplitudes.

DOI: 10.1103/PhysRevD.64.103001

PACS number(s): 98.70.Vc

I. INTRODUCTION

In the last few years there has been great surge of interest in the polarization anisotropies of the cosmic microwave background (CMB). The detection of CMB polarization anisotropies has become a major goal in our field, prompting many groups to build experiments and to start thinking about future satellite missions dedicated to polarization (see, for example, Refs. [1–4]).

The pattern of polarization on the sky can be characterized in terms of a scalar field (E) and a pseudoscalar field (B) [5,6]. This decomposition is particularly useful because density fluctuations cannot produce B type polarization [7,8]. A B type pattern is a direct signature of the presence of a stochastic background of gravitational waves. Such detection would provide invaluable information about inflation (for estimates of how constraints on parameters of the inflationary model would improve by measuring polarization; see, for example, Refs. [9–11]). This is perhaps the most important source for the new interest in polarization. It was also proposed that the detection of B polarization could signal other types of “new physics” [12].

The mathematics of the E - B decomposition was presented in several papers [5,6,13–15]. In this paper we will present a different derivation of the E - B transformation that will highlight the ingredients that are needed to connect the spin two fields of Q and U with the scalar and pseudoscalar fields E and B . The aim is to gain intuition into the E - B decomposition, which is particularly useful at this stage when new experiments are being designed. Intuition will help address issues such as the optimal shape of the sky patch needed to separate E from B , or if both Q and U Stokes parameters need to be measured.

We will also present the E and B decompositions of some simple polarized maps. Our aim is to understand if having a map with $B=0$, such as the one produced by density perturbation, is something generic or if one should always expect $E \approx B$.

The paper is organized as follow, in Sec. II we present a derivation of the E - B decomposition. In Sec. III we present the decomposition for some simple intensity and polarization maps. We comment on our observational strategies and conclude in Sec. IV.

II. GEOMETRICAL PROPERTIES OF THE E - B DECOMPOSITION

The CMB anisotropy field is characterized by a 2×2 intensity tensor I_{ij} . The intensity tensor is a function of the direction on the sky $\hat{\mathbf{n}}$ and two directions perpendicular to $\hat{\mathbf{n}}$ that are used to define its components ($\hat{\mathbf{e}}_1, \hat{\mathbf{e}}_2$). The Stokes parameters Q and U are defined as $Q = (I_{11} - I_{22})/4$ and $U = I_{12}/2$, while the temperature anisotropy is given by $T = (I_{11} + I_{22})/4$ (the factor 4 relates fluctuations in the intensity with those in the temperature, $I \propto T^4$). These three quantities fully describe any state of linearly polarized light. While the temperature is invariant under a rotation in the plane perpendicular to the direction $\hat{\mathbf{n}}$, Q and U transform under rotation by an angle ψ as

$$\begin{aligned} Q' &= Q \cos 2\psi + U \sin 2\psi, \\ U' &= -Q \sin 2\psi + U \cos 2\psi, \end{aligned} \quad (1)$$

where $\hat{\mathbf{e}}'_1 = \cos \psi \hat{\mathbf{e}}_1 + \sin \psi \hat{\mathbf{e}}_2$ and $\hat{\mathbf{e}}'_2 = -\sin \psi \hat{\mathbf{e}}_1 + \cos \psi \hat{\mathbf{e}}_2$.

It is useful not to describe the polarization field in terms of Q and U but to do so in terms of two quantities that scalar under rotation, usually called E and B [5,6]. This E - B decomposition is a linear transformation of the Q - U field on the sky. The transformation is invertible. E and B differ in their behaviors under a parity transformation: B changes sign while E does not.

To make our derivation more transparent we will work in the flat sky approximation, which is valid for small patches of sky. We do this only for the sake of clarity, as all of our results can be trivially generalized to a full sky analysis. In the flat sky limit the directions ($\hat{\mathbf{e}}_1, \hat{\mathbf{e}}_2$) used to define the Stokes parameters at every point in the plane of the sky correspond to the coordinate axis $(\hat{\mathbf{e}}_1, \hat{\mathbf{e}}_2) = (\hat{\mathbf{x}}, \hat{\mathbf{y}})$.

A general linear transformation can be written as

$$\begin{aligned} E(\boldsymbol{\theta}) &= \int d^2 \boldsymbol{\epsilon} \mathbf{K}_E(\boldsymbol{\theta}, \boldsymbol{\epsilon}) \mathbf{X}(\boldsymbol{\epsilon}) \\ B(\boldsymbol{\theta}) &= \int d^2 \boldsymbol{\epsilon} \mathbf{K}_B(\boldsymbol{\theta}, \boldsymbol{\epsilon}) \mathbf{X}(\boldsymbol{\epsilon}). \end{aligned} \quad (2)$$

where \mathbf{X} is the two component vector $\mathbf{X}=(Q,U)$, and $\mathbf{K}_{(E,B)}$ are transformation kernels.

We want to derive the properties that the kernels must satisfy to make E and B transform correctly. We first consider two types of transformations, a translation and a rotation. Under a translation by a distance θ_0 the vectors on the plane of the sky transform as $\theta' = \theta + \theta_0$. Under a rotation of the coordinate system by an angle ψ they transform as $\theta' = \mathbf{R}(\psi)\theta$, with \mathbf{R} the standard rotation matrix. The explicit convention for the rotation is explained below Eq. (1). In both cases E and B should remain unchanged; in other words,

$$\begin{aligned} E'(\theta') &= E(\theta) \\ B'(\theta') &= B(\theta) \end{aligned} \quad (\text{for translations \& rotations}). \quad (3)$$

Equation (3) implies that

$$\begin{aligned} \int d^2\epsilon \mathbf{K}_E(\theta', \epsilon) \mathbf{X}'(\epsilon) &= \int d^2\epsilon \mathbf{K}_E(\theta, \epsilon) \mathbf{X}(\epsilon), \\ \int d^2\epsilon \mathbf{K}_B(\theta', \epsilon) \mathbf{X}'(\epsilon) &= \int d^2\epsilon \mathbf{K}_B(\theta, \epsilon) \mathbf{X}(\epsilon). \end{aligned} \quad (4)$$

Under a translation Q and U are remain unchanged, $\mathbf{X}'(\theta') = \mathbf{X}(\theta)$. Equation (3) implies that $\mathbf{K}_{(E,B)}(\theta, \epsilon) = \mathbf{K}_{(E,B)}(\theta - \epsilon)$.

On the other hand, under a rotation Q and U are not scalars. They change as

$$\mathbf{X}'(\theta') = \mathbf{R}_X(\psi)\mathbf{X}(\theta), \quad (5)$$

with the matrix $\mathbf{R}_X(\psi)$ defined in Eq. (1). Equation (5) implies that the E - B decomposition has to be nonlocal. E and B at point θ cannot be constructed by combining Q and U at that same point, because any such linear combination (if invertible) would not be scalar under rotations.

The other type of transformation that needs to be considered are reflections. After a reflection E remains unchanged and B changes sign:

$$\begin{aligned} E'(\theta') &= E(\theta) \\ B'(\theta') &= -B(\theta) \end{aligned} \quad (\text{for parity}). \quad (6)$$

Although Eq. (6) is valid for any reflection, to be concrete we consider a reflection about the $\hat{\mathbf{y}}$ axis. The position vectors transform as $\theta' = (\theta'_x, \theta'_y) = (-\theta_x, \theta_y)$ and the Stokes parameters as $Q'(\theta') = Q(\theta)$ and $U'(\theta') = -U(\theta)$. The transformation laws for reflections about other axis can be obtained by combining these transformation laws with the transformation properties for rotations.

Rather than trying to find directly the form of the kernels needed to satisfy all the above properties, for pedagogical reasons we will use Figs. 1 and 2 to derive the kernels in a more intuitive way. We first consider the contribution to $E(\theta)$ from a point ϵ at a distance $\tilde{\theta}$ along $\hat{\mathbf{y}}$. We will assume that the contribution from this point is not zero. Note that with this particular configuration the axis $(\hat{\mathbf{e}}_1, \hat{\mathbf{e}}_2)$ at point ϵ

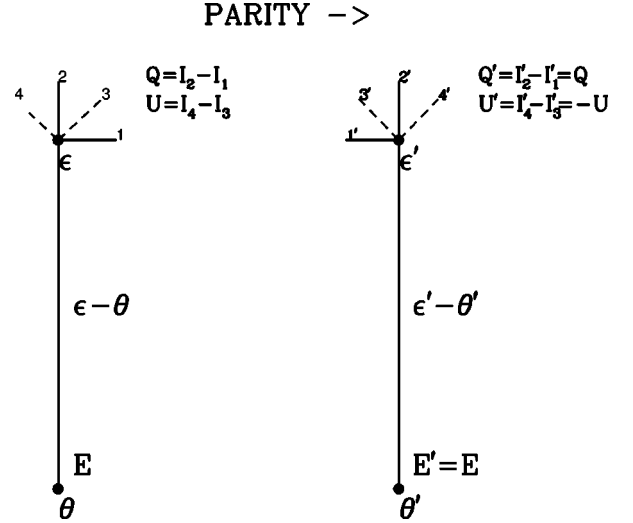


FIG. 1. Contribution to $E(\theta)$ from point ϵ . The two panels are related by a parity transformation, a reflection across the $\hat{\mathbf{y}}$ axis. The axes labeled by numbers are the ones used to define the Stokes parameters. In the flat sky limit, $(\hat{\mathbf{e}}_1, \hat{\mathbf{e}}_2) = (\hat{\mathbf{x}}, \hat{\mathbf{y}})$.

are aligned with the vector $\epsilon - \theta$. This is the reason we chose this setup. We will obtain the kernels for other configurations using the scalar nature of E under rotations.

The contribution to $E(\theta)$ from ϵ , which we will call $\delta E(\theta)$, is

$$\delta E(\theta) \propto \alpha_E^q Q(\epsilon) + \alpha_E^u U(\epsilon), \quad (7)$$

where we have introduced $\mathbf{K}_{(E,B)}(\tilde{\theta}\hat{\mathbf{y}}) = (\alpha_{(E,B)}^q, \alpha_{(E,B)}^u)$. E is invariant under reflections. In Fig. 1 we consider a reflection across the $\epsilon - \theta$ line, the $\hat{\mathbf{y}}$ axis. After this transformation $\theta' = \theta$ and $\epsilon' = \epsilon$ but the Stokes parameters change as $Q' = Q$ and $U' = -U$. This implies that $\alpha_u^E = 0$.

To construct a quantity that is invariant under parity (E), the contribution from a point separated by $\tilde{\theta}\hat{\mathbf{y}}$ can only in-

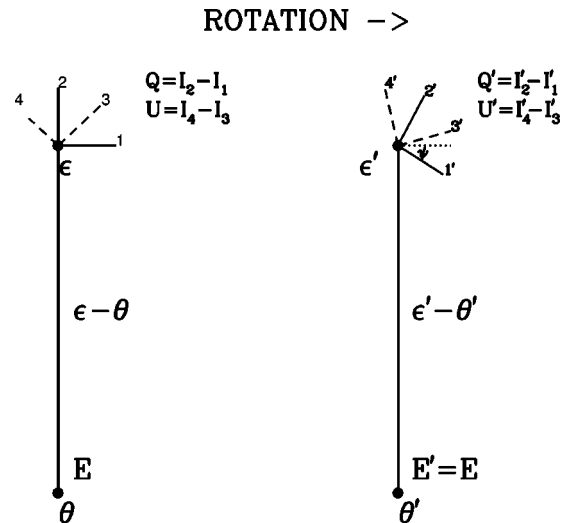


FIG. 2. Contribution to $E(\theta)$ from point ϵ . The two panels are related by a rotation by an angle ψ .

volve Q . Our conclusion is a consequence of the particular geometrical setup, but we will use the transformation properties under rotations to derive the kernels for other directions.

We use Fig. 2 to understand what happens under rotations. When we rotate the coordinate system by an angle ψ , the Stokes parameter are changed as described by Eq. (1). The position angle of point $\boldsymbol{\epsilon}$ with respect to the $\hat{\mathbf{x}}$ axis, which we will call $\tilde{\phi}$, changes from $\pi/2$ to $\pi/2 + \psi$. We have to allow for the kernels to depend on this position angle; otherwise E would never be a scalar under rotations given the transformation properties of Q and U . Using the above argument about parity, we concluded that

$$\begin{aligned}\alpha_q^E(\pi/2) &= \omega(\tilde{\theta}), \\ \alpha_u^E(\pi/2) &= 0,\end{aligned}\quad (8)$$

where we have called $\omega(\tilde{\theta})$ the value of the kernel at $\pi/2$. We have explicitly included a dependence on the separation $\tilde{\theta}$, because there is no reason why all the points along $\hat{\mathbf{y}}$ should contribute equally. E is a scalar, so

$$\delta E'(\boldsymbol{\theta}') = \delta E(\boldsymbol{\theta}),$$

$$\alpha_q^E(\pi/2 + \psi)Q' + \alpha_u^E(\pi/2 + \psi)U' = \omega Q. \quad (9)$$

This equation should be valid for arbitrary values Q and U . Combining Eqs. (1) and (9), we obtain

$$\begin{aligned}\alpha_q^E(\tilde{\phi}) &= -\omega(\tilde{\theta})\cos(2\tilde{\phi}), \\ \alpha_u^E(\tilde{\phi}) &= \omega(\tilde{\theta})\sin(2\tilde{\phi}).\end{aligned}\quad (10)$$

In fact, Eq. (10) is simple to interpret: only $Q_r = I_r - I_t$, the difference between the radial and tangential intensities can be used to construct E , and the weight can only depend on the distance $\tilde{\theta}$. In other words when constructing E at $\boldsymbol{\theta}$ we should use the radial and tangential unit vectors to define the Stokes parameters $(\hat{\mathbf{e}}_1, \hat{\mathbf{e}}_2) = (\hat{\mathbf{e}}_r, \hat{\mathbf{e}}_\phi)$. In this frame only Q_r contributes to E .

We have proven that $E(\boldsymbol{\theta})$ can be expressed as

$$\begin{aligned}E(\boldsymbol{\theta}) &= \int d^2\tilde{\boldsymbol{\theta}}\omega(\tilde{\theta})Q_r(\boldsymbol{\theta} + \tilde{\boldsymbol{\theta}}) \\ &= \int d^2\tilde{\boldsymbol{\theta}}\omega(\tilde{\theta})[Q(\boldsymbol{\theta} + \tilde{\boldsymbol{\theta}})\cos(2\tilde{\phi}) - U(\boldsymbol{\theta} + \tilde{\boldsymbol{\theta}})\sin(2\tilde{\phi})].\end{aligned}\quad (11)$$

Any choice of weight w will produce a quantity that is scalar under rotation and invariant under parity.

A similar argument can be used to show that the only way to construct B , a quantity invariant under rotations but that changes sign under reflections is

$$\begin{aligned}B(\boldsymbol{\theta}) &= \int d^2\tilde{\boldsymbol{\theta}}\omega(\tilde{\theta})U_r \\ &= \int d^2\tilde{\boldsymbol{\theta}}\omega(\tilde{\theta})[Q(\boldsymbol{\theta} + \tilde{\boldsymbol{\theta}})\sin(2\tilde{\phi}) + U(\boldsymbol{\theta} + \tilde{\boldsymbol{\theta}})\cos(2\tilde{\phi})],\end{aligned}\quad (12)$$

where now U_r is the U Stokes parameter defined with respect to the radial and tangential directions. In general ω in Eqs. (11) and (12) need not be the same.

The usual definition of E and B corresponds to a particular choice of the weight ω :

$$\omega(\tilde{\theta}) = -1/\tilde{\theta}^2 (\tilde{\theta} > 0) \quad (13)$$

[$\omega(0) = 0$; but as will become apparent later this fact is not important for smooth fields]. There are several reasons why this choice is made, some of which are easier to understand when working in Fourier space. As Eqs. (11) and (12) make clear, the E - B transformation is a convolution and thus becomes a multiplication in Fourier space. The choice of ω is such that the relation between E - B and Q - U is a simple rotation in Fourier space with no scale dependent factor. With ω given in Eq. (13), the relations are

$$\begin{aligned}Q(\boldsymbol{l}) &= [E(\boldsymbol{l})\cos(2\phi_l) - B(\boldsymbol{l})\sin(2\phi_l)], \\ U(\boldsymbol{l}) &= [E(\boldsymbol{l})\sin(2\phi_l) + B(\boldsymbol{l})\cos(2\phi_l)].\end{aligned}\quad (14)$$

Furthermore, with these choices the ensemble average of $P = Q^2 + U^2$ is the same as the ensemble average of $E^2 + B^2$. The sign convention on the other hand is chosen so that positive values of E generate a tangential pattern of polarization. The convention is rooted in the weak lensing literature which has identical mathematics and where the E field corresponds to the projected density κ which produces tangential distortions when positive.

For the purpose of finding a linear combination of Q - U that tests for the presence of gravitational waves or B type polarization any choice of ω is equally good. Other practical considerations such as the geometry of the observed patch of sky will probably be more important. In weak lensing there is a long literature that deals with different choices of ω , to create, for example, measures of the enclosed mass that are more local than the $1/\theta^2$ weighting. It is beyond the scope of this section to summarize that literature. We want the reader to take away three basic points from the above exercise.

The construction of E and B out of Q and U is by its very nature nonlocal.

To construct scalars under rotation at point $\boldsymbol{\theta}$ we need to average the Stokes parameters around circles centered at $\boldsymbol{\theta}$ using the radial and tangential directions of this circle to define the Stokes parameters (Q_r, U_r) . The weight along the circle should be constant.

To construct E (a scalar) we need to average Q_r and to construct B (a pseudoscalar) we need to average U_r .

III. EXAMPLES

In this section we consider simple intensity-polarization maps to illustrate some of the properties of the E - B decomposition. As a byproduct we will understand better if the fact that density perturbations produce only E type polarization is a unique prediction or if most sources of polarized emission have this characteristic.

A. Simple maps

We start by considering a localized source of radiation of typical extent L and centered around the origin. We first intend to compute the E - B fields for points far away from this distribution. In this limit, Eqs. (11) and (12) become

$$\begin{aligned} E(\boldsymbol{\theta}) &= \frac{\cos(2\phi)}{\theta^2} \int d^2\tilde{\boldsymbol{\theta}} Q(\tilde{\boldsymbol{\theta}}) - \frac{\sin(2\phi)}{\theta^2} \int d^2\tilde{\boldsymbol{\theta}} U(\tilde{\boldsymbol{\theta}}), \\ B(\boldsymbol{\theta}) &= \frac{\sin(2\phi)}{\theta^2} \int d^2\tilde{\boldsymbol{\theta}} Q(\tilde{\boldsymbol{\theta}}) + \frac{\cos(2\phi)}{\theta^2} \int d^2\tilde{\boldsymbol{\theta}} U(\tilde{\boldsymbol{\theta}}). \end{aligned} \quad (15)$$

The choice of ω implies that the amplitude of E and B decay as $1/\theta^2$. What is more interesting is that whether E or B are different from zero depends on the direction of observation. In fact there is no way to make B zero everywhere and keep E different from zero. E and B are only zero everywhere if the source is not polarized on average.

In the case where the average polarization is along the $\hat{\mathbf{x}}$ or $\hat{\mathbf{y}}$ axis, E and B are

$$\begin{aligned} E(\boldsymbol{\theta}) &= \frac{\cos(2\phi)}{\theta^2} \bar{Q} \Omega_s, \\ B(\boldsymbol{\theta}) &= \frac{\sin(2\phi)}{\theta^2} \bar{Q} \Omega_s, \end{aligned} \quad (16)$$

where \bar{Q} gives the average polarization of the source and Ω_s is the solid angle it subtends. The direction dependence of E - B can be easily understood in terms of parity transformations. The mean polarization is invariant under reflections along directions where $B=0$ and changes sign along directions where $B \neq 0$.

As we discussed in Sec. II, the E - B transformation has to be nonlocal. This implies that a localized source of emission will produce E - B even outside the region where Q and U are not zero. Our simple exercise has shown that if the source has a mean polarization, the typical sizes of the E and B components are the same outside the source.

Let us now consider points inside the source. The first potential problem is that the weight function seems to diverge at zero distance. We consider a smooth Q - U field that can be expanded in Taylor series. We assume we are calculating E and B at point $\boldsymbol{\theta}$ and we expand Q and U around that point:

$$Q(\boldsymbol{\theta} + \tilde{\boldsymbol{\theta}}) = Q|_{\boldsymbol{\theta}} + \tilde{\theta}_i U_{,i}|_{\boldsymbol{\theta}} + \frac{1}{2} \tilde{\theta}_i \tilde{\theta}_j Q_{,ij}|_{\boldsymbol{\theta}} \dots,$$

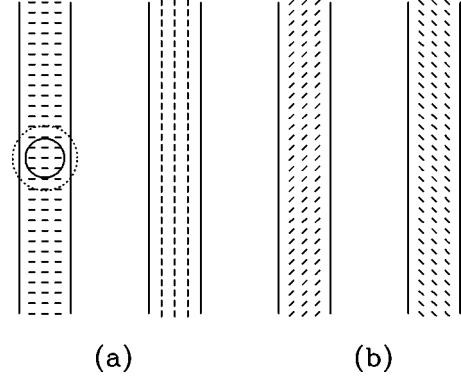


FIG. 3. Examples of polarization vectors inside filaments. The two circles indicate points that contribute with equal weights to E and B at the center of those circles. The contributions from points along the smaller circle cancel as one moves along the circle. The contribution from the second circle is different from zero. In the case shown the contribution is mainly E . The first two filaments [labeled (a)] produce mainly E type polarization inside the filaments, while the second two [labeled (b)], produce mainly B type polarization.

$$U(\boldsymbol{\theta} + \tilde{\boldsymbol{\theta}}) = U|_{\boldsymbol{\theta}} + \tilde{\theta}_i U_{,i}|_{\boldsymbol{\theta}} + \frac{1}{2} \tilde{\theta}_i \tilde{\theta}_j U_{,ij}|_{\boldsymbol{\theta}} \dots, \quad (17)$$

where we denote derivatives with respect to the different coordinates as $,i$, and a summation of indices is implied. To compute E and B we replace Eq. (17) into Eqs. (11) and (12). The first terms to contribute are the second order ones because of the $\cos(2\tilde{\phi})$ and $\sin(2\tilde{\phi})$ factors in Eqs. (11) and (12). $1/\tilde{\theta}^2$ in $\omega(\tilde{\boldsymbol{\theta}})$ is canceled by $\tilde{\theta}^2$ coming from the Taylor expansion. In fact there is an extra $\tilde{\theta}$ from the $d^2\tilde{\boldsymbol{\theta}}$; there is no divergence at the origin. We also conclude that E and B are most sensitive to the ‘‘quadrupole’’ pattern around $\boldsymbol{\theta}$; the quadratic term in the Taylor expansion.

As an example we can consider a filament, as shown in Fig. 3. The emitting region has a length L along the $\hat{\mathbf{y}}$ axis and a width l along the $\hat{\mathbf{x}}$ axis ($L \gg l$). We will assume that the Stokes parameters are constant along the filament and are zero outside.

We now imagine doing the integrals in Eqs. (11) and (12) one circle at a time. As long as the radius of the circle is smaller than l the angular integrals cancel. It is an easy exercise to compute the values of E and B at the center of the filament,

$$\begin{aligned} E &= -cQ, \\ B &= -cU, \end{aligned} \quad (18)$$

$$c = 4 \int_1^{L/l} dx \sqrt{\frac{x^2 - 1}{x^3}},$$

where $x = \tilde{\theta}/l$. Equation (18) shows that E and B only receive contributions from rings larger than l , and that the maximum contribution comes from $\theta \approx \sqrt{3/2}l$. The contribution from far away rings are down by $1/\tilde{\theta}^2$.

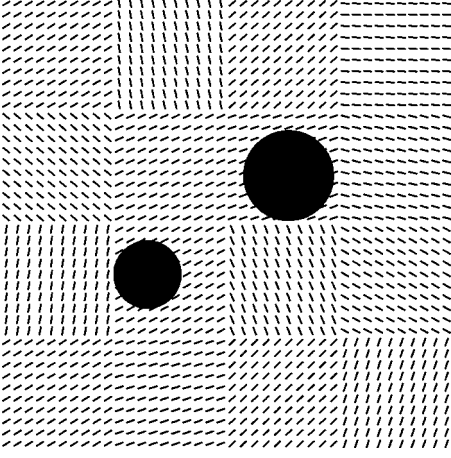


FIG. 4. For illustration purposes we show a random pattern of polarization with a coherence length we call L . For the two points at the center of the filled circles, only the regions outside the circles contribute. External patches contribute on average the same to E and B . Only points inside the patch (but outside the circles) will contribute dominantly to E or to B . Which contribution is larger depends on the orientation of the polarization inside the patch and the position of the point where E and B are being calculated.

Although we have presented a very simplified example, we see two important features of the E - B transformation. If the Q - U fields are constant over a scale l , rings smaller than this do not contribute to E or B . Around a particular point, if the polarization vectors tend to be aligned or are perpendicular to the direction over which magnitude of the polarization is changing the pattern has a larger E than B . To have B the pattern has to form an angle of approximately 45° with that direction. In the case of a filament this is illustrated in Fig. 3.

Finally we consider a case in which the polarization pattern is very random, formed by regions of finite extent of typical size L inside which the polarization is constant. Different patches are independent. We sketch such a pattern in Fig. 4. We want to know how the typical values E and B at a point θ inside a particular region compare. From our above examples we can conclude that the contributions to E and B coming from external patches are statistically the same; they depend, for any particular external patch, on the relative orientation of the polarization in that patch and the separation vector $\tilde{\theta}$. The contributions from points inside the same patch cancel to a great extent, but some E and B are left. Which dominates at a particular θ again depends on the relative orientation of the polarization and the separation vector between θ and the center of the patch. Thus for a random pattern we expect similar levels of E and B .

Our final example argues that for polarization patterns that have a finite coherence length one should expect to have roughly the same E and B . This shows how remarkable it is that density perturbations do not produce any B modes. In order for B to be zero, the integral of U_r has to vanish identically (not just statistically) for every possible ring around any point, regardless of the radius of the ring. It is clear that this important symmetry will not hold for most random processes.

B. Supernova remnant

In this section we consider a more realistic model for polarized emission, a model for the emission of a supernova remnant (SNR) [16]. This has been used successfully to model the emission from the galactic spurs at radio frequencies around 1.4 GHz.

The basic features of the model can be summarized as follows. Radiation is produced by synchrotron emission from a shell. The thickness of the shell depends on position and (to first order in the shell thickness) is given by

$$\epsilon(\psi) = \Delta r/r = \bar{\epsilon} \sin(\psi) \quad (19)$$

where r is the radius of the shell, ψ is the angle relative to the direction of the initial magnetic field, and $\bar{\epsilon}$ is the maximum thickness of the shell.

The interstellar magnetic field had a strength B_0 before the supernova explosion. Later it is oriented along the surface of the shell and is amplified to a value $B = B_0/2\bar{\epsilon}$, a consequence of flux conservation. This model assumes that energy distribution of the particles responsible for the emission is of the form

$$N(E)dE = KE^{-\gamma}dE. \quad (20)$$

Moreover, it assumes equipartition between the energy density in particles and magnetic fields:

$$K \int_{E_{\min}}^{E_{\max}} E^{-\gamma+1} dE \sim \frac{B^2}{8\pi}. \quad (21)$$

Detailed derivations of these equations as well as parameters that can fit different structures in our galaxy can be found in Refs. [16,17]. It is not our objective to analyze what is expected from particular structures in our galaxy, but rather to use this model to make a map of polarization and compute its E - B decomposition to help build intuition. For this purpose the only two relevant parameters are the angle (β) between the plane of the sky and the unperturbed interstellar magnetic field (\mathbf{B}_0) and the maximum width of the shell $\bar{\epsilon}$. Without loss of generality we will assume that \mathbf{B}_0 lies in the \mathbf{x} - \mathbf{z} plane (the \mathbf{x} - \mathbf{y} plane is the plane of the sky). The projection on the sky of the unperturbed field is $B_0 \cos(\beta)$.

We then compute the intensity and polarization observed along each line of sight by integrating the synchrotron emissivity along the line of sight,

$$\begin{aligned} I &= A \int dx B_{\perp}^{(\gamma+1)/2}, \\ Q &= A \Pi \int dx B_{\perp}^{(\gamma+1)/2} \cos(2\phi), \\ U &= A \Pi \int dx B_{\perp}^{(\gamma+1)/2} \sin(2\phi), \end{aligned} \quad (22)$$

where Π is the degree of polarization of the synchrotron emission, B_{\perp} is the component of the local magnetic field on

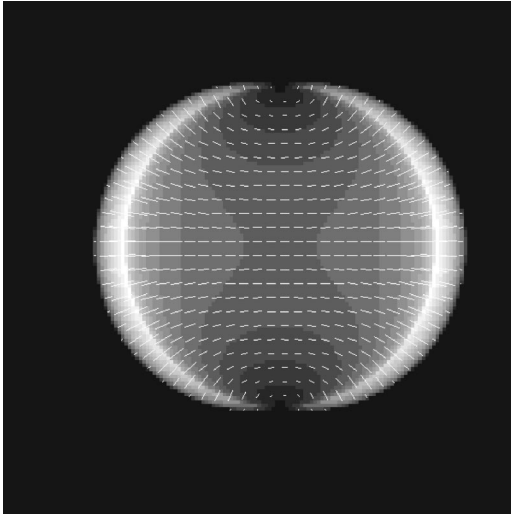


FIG. 5. Temperature and polarization map for a model of SNR with $\beta=45^\circ$. Rods indicate a magnitude of $P=Q^2+U^2$.

the plane of the sky, ϕ is the angle between \mathbf{B}_\perp and the \mathbf{x} axis, and A is a normalization constant that depends on several parameters such as the number density of particles.

Figure 5 shows the intensity and polarization map for the case $\beta=45^\circ$. In Figs. 6 and 7 we show the corresponding E - B maps. E and B extend outside the remnant. The intensity and polarization map has symmetries of reflection across the $\hat{\mathbf{x}}$ and $\hat{\mathbf{y}}$ axes. The E map respects those symmetries, while the B map does not. The B maps changes sign as one moves across the $\hat{\mathbf{x}}$ and $\hat{\mathbf{y}}$ axes.

To understand the behavior of the Stokes parameters and the E and B fields, we will look at one dimensional cuts along the $\hat{\mathbf{x}}$ axis (perpendicular to the magnetic field). We show several examples in Fig. 8. Each of the columns corresponds to a cut at a different height along the remnant. From Fig. 8 we can conclude the following.

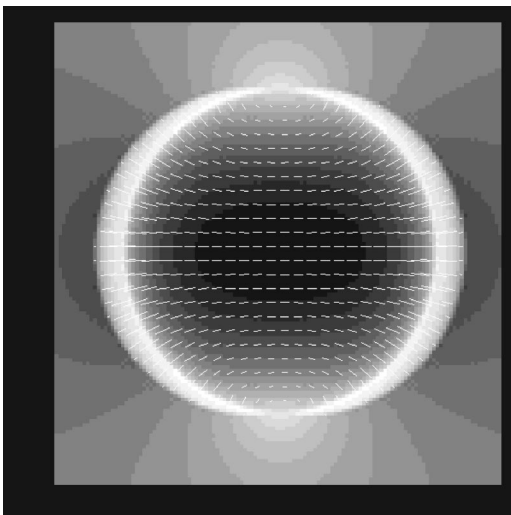


FIG. 6. E type polarization for a model of the SNR with $\beta=45^\circ$.

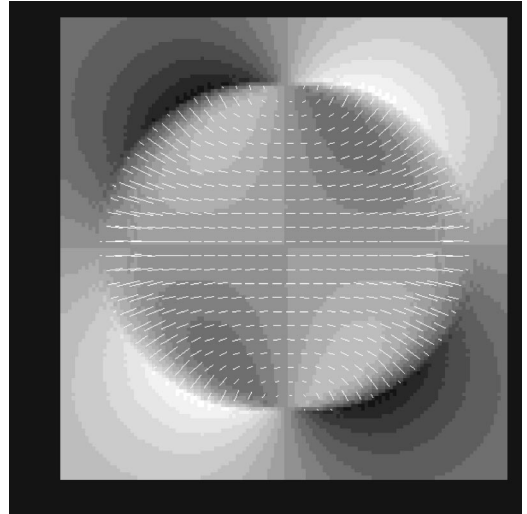


FIG. 7. B type polarization for a model of the SNR with $\beta=45^\circ$.

Both E and B extend outside the remnant and decay as $1/\theta^2$.

The temperature and polarization patterns are invariant under reflections across both the $\hat{\mathbf{x}}$ and $\hat{\mathbf{y}}$ axes. This implies that B is zero along both axes. E is invariant under reflections across the $\hat{\mathbf{x}}$ and $\hat{\mathbf{y}}$ axes but B changes sign.

Both E and B tend to peak at the edges of the SNR, where the T and P peak. We could think of the edge of the SNR as an example of the more idealized “filament” that we considered in the previous section. For $\beta=0^\circ$ and 45° we find that

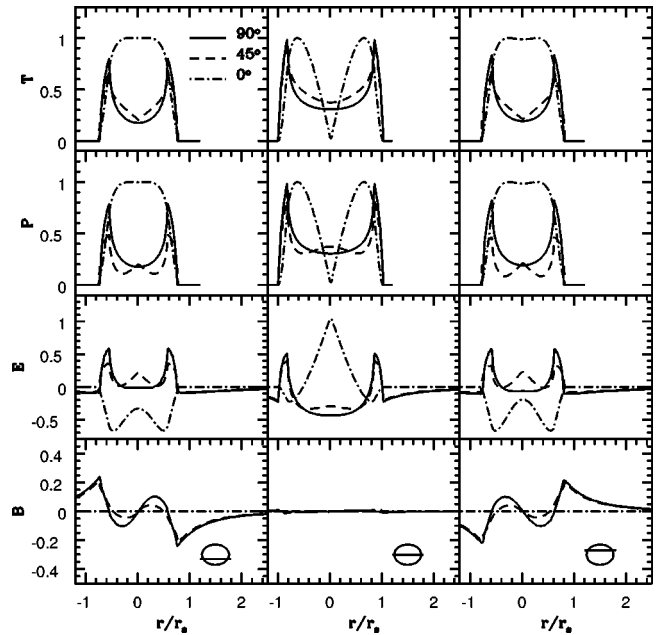


FIG. 8. One dimensional cuts of T , $P=\sqrt{Q^2+U^2}$, E , and B across SNR models. Each of the three columns corresponds to a different height $y=(-0.6,0,0.6)$ in units of the radius. In each panel we show the results for three different values of $\beta=(0,45,90)^\circ$. The E curve for $\beta=90^\circ$ and $y=0$ has been divided by a factor of 10, so all curves in the panel are visible.

E is positive at the peaks, that means that the polarization direction is perpendicular to the direction of the “filament.” For $\beta=90^\circ$ the situation is the opposite, and the polarization is parallel to the filament direction.

E is larger than B by a factor of a few in a “typical” place inside the ring of maximum emission. In particular, at the edges of the SNR, this means that the polarization is typically like patterns (a) of Fig. 4 rather than patterns (b).

If $\beta=90^\circ$ B is zero everywhere because the polarization pattern has reflection symmetry across any axis going through the origin.

If $\beta=90^\circ$ the E component has a very large peak at the origin because the pattern is circular around that point. Note that there is no emission ($T=P=0$) at the origin, where E has the maximum. This illustrates the fact that one cannot define a degree of polarization using E and B , because their relation to Q and U is not local.

It is important to realize that many of our conclusions follow from specific symmetry properties of the source. In reality these symmetries will be broken by real world complications such as inhomogeneities in the density or magnetic fields. As our examples in Sec. II show, as the symmetries are lost the amplitudes of E and B become more similar. Moreover, because the E - B transformation is nonlocal, if only part of the SNR is in the observed field, the E and B decompositions will be different.

IV. DISCUSSION

Detecting a B component in the CMB polarization field would be a great triumph for cosmology. As discussed above, the transformation between Q - U and E - B is necessarily non-local. Moreover, just from geometrical requirements the only way to construct scalar and pseudoscalar quantities is to average Q_r and U_r over circles. Thus the geometry of the patch of sky to be observed should be such as to allow for many different circles to be inscribed.

The first generation of modern experiments, [1,3] measured the Stokes parameters in a ring on the sky. Thus only one circle can be constructed, and so, even if both Q and U are measured at every pixel along the ring, there is only one possible linear combination of the data that measure only E (the average of Q_r along the ring) and one linear combination that measures only B (the average of U_r along the ring). All other combinations of the data receive contributions simultaneously from both E and B . In practice Ref. [3] could

not use these combinations because $1/f$ noise makes them unreliable.

In general, one cannot construct circles around the points in the edge of the observed patch. Thus if the aim is to have the most possible linear combinations that are sensitive to either E or B but not to both, the best strategy is to make the observed patch of sky as round as possible.

Another consideration is that for each point where E and B are calculated one needs to average either Q or U in the natural frame, the radial and tangential directions. This means that in order to be able to do it for as many circles as possible, one has to measure both Q and U in every pixel.

The emphasis of our paper was to find linear combinations of Q and U that contain information about E or B alone. However it is perfectly possible to distinguish E and B type polarizations from the correlation functions of Q and U . Formulas that relate the power spectrum of E and B with the correlation functions of Q and U can be found, for example, in Ref. [5]. Distinguishing E and B this way does not rely on the shape of the observed region, as the correlation functions can be calculated just using pair of points.

However, one should realize that obtaining constraints on B from correlation functions comes at the price of larger error bars. It is clear that even though one can estimate the power spectrum this way, the errors in an estimate of B receive contributions from the power in both E and B type polarizations. Thus, because we expect the B signal to be smaller than the E signal, it is much better to directly find a linear combination (rather than quadratic combinations) of data that measure B . Suggestions of practical ways of separating E and B from correlation data were recently presented in Ref. [18]. In reality a full analysis such as the one described in Ref. [15] will incorporate all the information available in a given experiment, and should be preferred.

We have also analyzed the E and B patterns expected for simple maps. We argued that in general one expects both E and B type polarizations to have comparable amplitudes although not necessarily equal amplitudes. Whether E or B dominates at a particular place inside the source depends on the symmetries of the source. The E and B transformations are not local, so some E 's and B 's “leak” outside the source, unless the source is unpolarized on average. The amplitudes of E and B are the same outside the source, on average; however, which dominates at a particular point depends on the relative orientation between the polarization direction and the separation vector.

-
- [1] B. Keating, P. Timbie, A. Polnarev, and J. Steinberger, *Astrophys. J.* **495**, 580 (1998).
 [2] S. T. Staggs *et al.*, astro-ph/9904062.
 [3] M. M. Hedman, D. Barkats, J. O. Gundersen, S. T. Staggs, and B. Winstein, *Astrophys. J. Lett.* **548**, L111 (2001).
 [4] J. B. Peterson *et al.*, astro-ph/9907276.
 [5] M. Kamionkowski, A. Kosowsky, and A. Stebbins, *Phys. Rev. D* **55**, 7368 (1997).
 [6] M. Zaldarriaga and U. Seljak, *Phys. Rev. D* **55**, 1830 (1997).
 [7] M. Kamionkowski, A. Kosowsky, and A. Stebbins, *Phys. Rev. Lett.* **78**, 2058 (1997).
 [8] U. Seljak and M. Zaldarriaga, *Phys. Rev. Lett.* **78**, 2054 (1997).
 [9] M. Zaldarriaga, D. N. Spergel, and U. Seljak, *Astrophys. J.* **488**, 1 (1997).
 [10] M. Tegmark, D. J. Eisenstein, W. Hu, and A. de Oliveira-Costa, *Astrophys. J.* **530**, 133 (2000).
 [11] W. H. Kinney, *Phys. Rev. D* **58**, 123506 (1998).

- [12] A. Lue, L. Wang, and Marc Kamionkowski, Phys. Rev. Lett. **83**, 1506 (1999).
- [13] W. Hu and M. White, Phys. Rev. D **56**, 596 (1997).
- [14] M. Zaldarriaga, Astrophys. J. **503**, 1 (1998).
- [15] M. Tegmark and A. de Oliveira-Costa, Phys. Rev. D **64**, 063001 (2001).
- [16] H. van der Lann, Mon. Not. R. Astron. Soc. **124**, 125 (1962).
- [17] T. A. Th. Spoelstra, Astron. Astrophys. **21**, 61 (1972).
- [18] R. G. Crittenden, P. Natarajan, U. L. Pen, and T. Theuns, astro-ph/0012336.